Research Open

Geology, Earth and Marine Sciences
Volume 1 Issue 1

Research Article

Seismicity of Antarctica: Features

Khavroshkin OB[1]*, Khrustalev AB[2] and Tsyplakov VV[2]

Graduate engineer from Ecole Polytechnique. Promotion 1945, Knight of the Legion of Honor and the National Order of Merit Maurice Allais Award

Corresponding Author: Khavroshkin OB, Professor, Department of Geophysical Methods, Schmidt Institute of Physics of the Earth of the Russian Academy of Sciences, Russia; **Tel:** ; **Fax:** ; **E-mail:** khavole@ifz.ru

Received: October 21, 2019; **Accepted:** November 11, 2019; **Published:** November 21, 2019

Abstract

In this paper, the spectral characteristics of seismic data obtained at various seismic stations in Antarctica are studied using the spectral histogram method developed by the authors and the study of regional structures. This takes into account the fundamental features of the geological, geophysical and astrophysical picture of the entire continent; significant component of fragile crustal structures. The possibility of the existence in the polar region of the ancient structures of the plume during its formation experienced the impact of centrifugal forces from the rotation of the Earth and the inhibition of the top of the plume in the low-temperature near-surface layer. One of the most significant attractions of the region is the existence of a large-sized ozone "hole". All the above features have found their reflection in the seismic fields of Antarctica.

Keywords: *Antarctica, seismic fields, plume tectonics, ozone holes, modulated solar wind, solar oscillations*

Introduction

Probable plume tectonics It is likely that the Antarctic bears the signs of a super plume (Fig. 1). A similar example of a modern "hot spot" is about. Iceland. The thickness of the ocean-type crust under this island reaches 40 km. (usually the thickness is 7 km). Paleo - Iceland's counterparts - a giant Antarctic uplift, etc. Until now, volcanic activity has been observed in Antarctica (Figure 1).

Figure 1. There is an example of the plume development. At the final stage, the tip of the Antarctic plume, due to the anomalously cooled surface rocks of the crust, will assume a more subtle and probably not continuous form.

The modern map of Antarctica quite well shows similarities with the elements of the super - plume (Fig. 2.) (Figure. 2a,b).

Given the thickness of the ice cover (up to 9 km), and the structure of the crustal rocks, as well as thermal and coastal processes, we should expect the existence of various seismic fields. In addition, there are many caves in the coastal zone, possibly remnants from the periphery of the plume. During the Second World War, a submarine base of Germany existed in the caves off the coast. There is the existence of the ozone hole over the continent. Large-scale, ozone-free atmospheric space above the continent (Figure 3) makes radical additions to the description of Antarctic seismicity. There are such effects that are impossible for terrestrial seismicity. The absence of ozone protection makes available the effect on the surface of many solar processes: radiation (from ultraviolet radiation to x-rays and gamma radiation), solar cosmic rays and flares, muons, modulated solar wind and interplanetary shock waves (MUV). A similar picture is observed for lunar seismicity. Many of the effects are almost constantly modulated, for example, by solar oscillations which make it possible to observe waves at solar frequencies in the spectrum of the seismic field (Table 1).

Antarctica

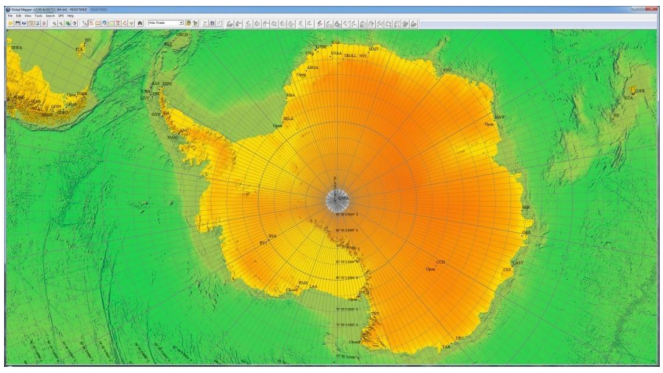

A

B

Figure 2. A, B. This is modern map of Antarctica. With the exception of the peninsula, the coasts are rounded, forming a super plume.

In Table 1: p, g, f-modes of the natural oscillations of the Sun; L-form of natural oscillations.

Moreover, the excitation of these waves is not due to the indirect interaction of terrestrial radioactive geological structures with solar neutrinos, but directly. This means that instrumental and methodological development of seismic expeditions to the Moon, Mars and other space bodies devoid of ozone protection should be carried out on Antarctica, as the closest to the external conditions of the landfill (Figure 3).

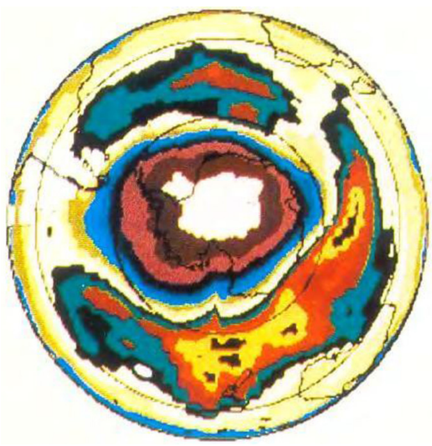

Figure 3. Map of the ozone hole over Antarctica.

The ozone hole over the Antarctic and its adjacent territories is quite dynamic: it grew for the first time in recent years, covering an area of 28 million square kilometers (press service of the NASA Goddard Space Flight Center). Previously, the ozone layer was considered to be a natural shield that protects the surface of the Earth from hard ultraviolet radiation, which is dangerous to living organisms. Now it is a parameter of the atmosphere, which allows studying the Sun, solar-terrestrial relations and some astrophysical problems. A sharp drop in the concentration of stratospheric ozone during the winter season was first detected over the Antarctica in the 1980s. Every winter, the ozone hole over Antarctica grows, reaching a maximum area in September, and shrinking in summer. Large sizes fully correspond to how ozone behaves in relatively cold weather in the upper atmosphere of the Earth (Paul Newman, Paul Newman, USA). Due to the slow reduction, the thickness of the ozone layer in some deep regions of the Antarctic has fallen to absolute zero for the first time in many years. This means that the Suns freely “bombard” the polar ice that is under similar areas, for example, the Amundsen – Scott station at the South Pole. The level of ozone began to fall sharply in September, with the result that its concentration decreased by 95% by the first of October. This year, the fall continued for two “extra weeks”, which led to a 100% decrease in the level of ozone by October 15”says another climatologist, Brian Johnson, USA. However, the smaller ozone hole in 2017 is the result of natural variability and is not necessarily a signal of rapid “healing”. Scientists use the word “hole” as a metaphor for an area in which the ozone concentration falls below the historical threshold of 220 Dobson units. A sharp drop in the concentration of stratospheric ozone during the winter season was first discovered over Antarctica in the 1980s. The reason for this was the release of a large number of Freon’s into the atmosphere of the Earth, whose molecules destroy ozone in the upper layers of the atmosphere at low air temperatures. Every winter, the ozone hole over Antarctica grows, reaching a maximum area in September, and shrinking in summer. January 29, 2016, 14:31 - January 27, a huge ozone hole covered northern Eurasia from the Atlantic to the Pacific Ocean. Most of it fell on the territory of Russia. The anomaly center is located in the north of Western Siberia, however, the effect of ozone holes is not yet known to seismologists. Observations in 2017 showed that the hole in the ozone layer of the Earth, which forms over Antarctica at the end of the southern winter, has become the smallest since 1988. According to NASA satellites, the ozone hole reached its one-year maximum of September 11, spreading to 7.6 million square miles (19.6 sq. km), which is 2.5 times the area of the United States. Ground-based measurements and measurements from balloons, carried out by the National Oceanic and Atmospheric Administration, confirmed satellite data. Since 1991, the average maximum area of ozone holes has been approximately 26 million square kilometers (Fig. 4.) (Figure 4).

In view of the above, a start was made to study the seismic fields of Antarctica (Figure 5).

As follows from Figure 5, considerable seismic material has been collected and processed, primarily relating to the coastal zone and partly of the shelf The IRIS Data Management Center (IRISDMC): http://service.iris.edu/fdsnws/dataselect/1/. The study of data was started with spectral analysis (see Fig. 6) (Figure 6).

Table 1. Periods of oscillations of the standard model of the Sun with the relative content of heavy elements Z = 0.02 according to calculations by Iben n Makhefi

Mode	Period (min)					Mode	Period (min)			
	l=0	*l=1*	*l=2*	*l=3*	*l=4*		*l=1*	*l=2*	*l=3*	*l=4*
p1	62,29	57,25	42,50	39,53	37,58	*f*		45,90	40,97	38.82
p2	40,94	36,98	32,19	29,42	27,62	*g1*	61,58	55,05	47.94	44,15
P3	30,93	27,88	25,09	23,21	21,92	*g2*	84,4	63.03	54.88	49,59
p4	24,49	22,30	20,52	19,26	18,31	*g 3*	105,3	72,58	61.88	57,73
p5	20,19	18,08	17,39	16,44	15,72	*g 4*	127,3	83,49	67,78	61,11
p6	17,17	16,04	15,10	14,38	13,81	*g 5*	148.2	95.38	74,9	64,89
p7	14,93	14,08	13,35	12,77	12,32	*g 6*	171,1	107,7	88,1	70,30
p8	13,21	12.55	11,97	11,51	11,14	*g 7*		120,2	91,8	76.83
p9	11,85	11,34	10,87	10,49	10,18	*g 8*		132.9	100,7	83.62
p10	10,78	10.35	9,97	9,85	9,39	*g 9*		145.9	109,7	90,56
p11	9,90	9,54	9.21	8.94	8,71	*g 10*		158,9	118,9	97,62
p12	9.15	8,84	8,56	8,32	8,11	*g 11*		172.1	128,1	104,5
p23	8,50	8,25	7,99	7.78	7.60	*g 12*			137,8	111,7
p14	7.94	7,71	7,49	7,31	7,15	*g 23*			147,0	118,9
p15	7.45	7,25	7,06	6,89	6,75	*g 14*			156.5	126,5
p16	7.02	6,84	6,67	6,52	6,39	*g 15*			166,7	133,3
p17	6.64	6,47	6,32	6,18	6,06	*g 16*			175,9	141,5
p18	6.39	6.14	6,00	5,87	5,77	*g 17*				148,6
p19	5.98	5,84	5,71	5,60	5,50	*g 18*				156,4
p20	5.69	5,58	5,45	5.34	5.25	*g 19*				164,0
						g 20				171,1

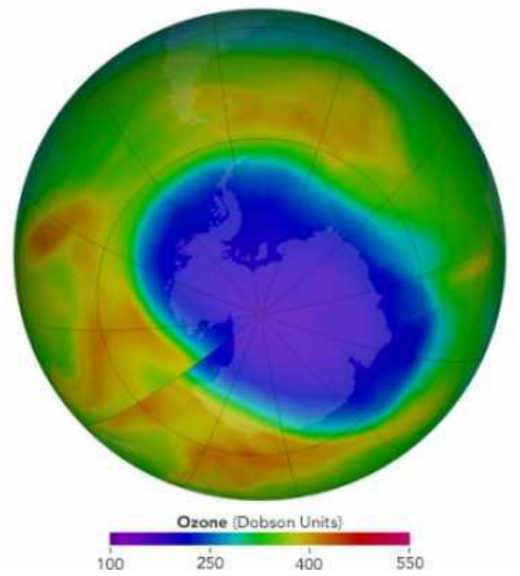

Figure 4. Concentration of ozone over Antarctica. October, 2017. © NASA

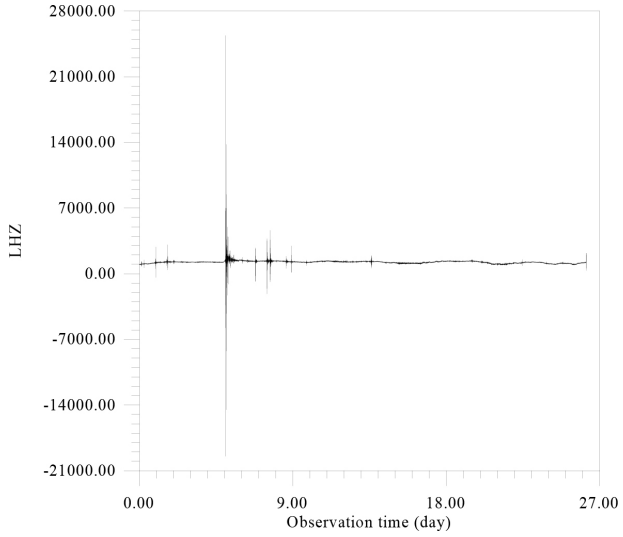

Figure 5. Seismic recording of LHZ-component 60 channel Streckeisen STS-2.5 sensor IU network of QSPA station (89.9289°S, 144.4382°E). The record contains 2265013 seconds. For convenience, the graphical representation is averaged over 120 points in 1 minute increments.

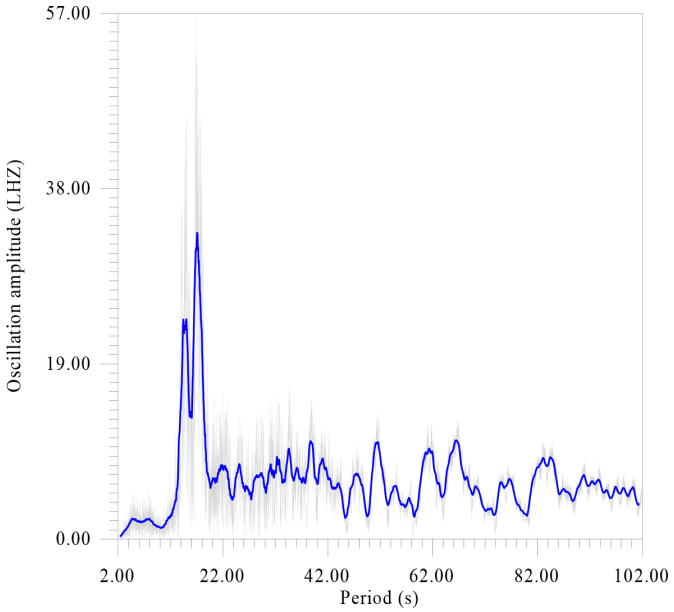

Figure 6. There is amplitude spectrum of seismic data in the range from 2 to 102 sec. in increments of 0.01 seconds. with averaging values of 1 sec.

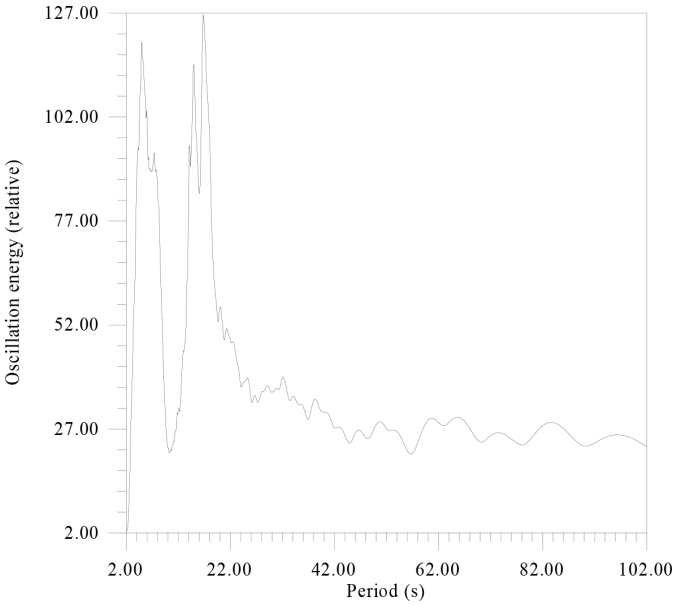

Figure 7. There is the energy spectrum of data Figure 6.

According to fig.6 the spectrum of seismicity has two peaks dominant in amplitude, for 18 and 20 sec., which, probably, given the proximity of the ocean, should be referred to as "storm" and note also the existence of resonant structures at the Antarctic ice sheet (Figure 7).

The energy spectrum revealed a more subtle structure of the peaks, at 4 and 18 sec. These peaks are not uncommon when considering seismic fields of complexly constructed and non-linear structures. For greater clarity, the same seismic material was processed by a more complex, but informative method (Fig.8 A, B) (Figure 8 a,b).

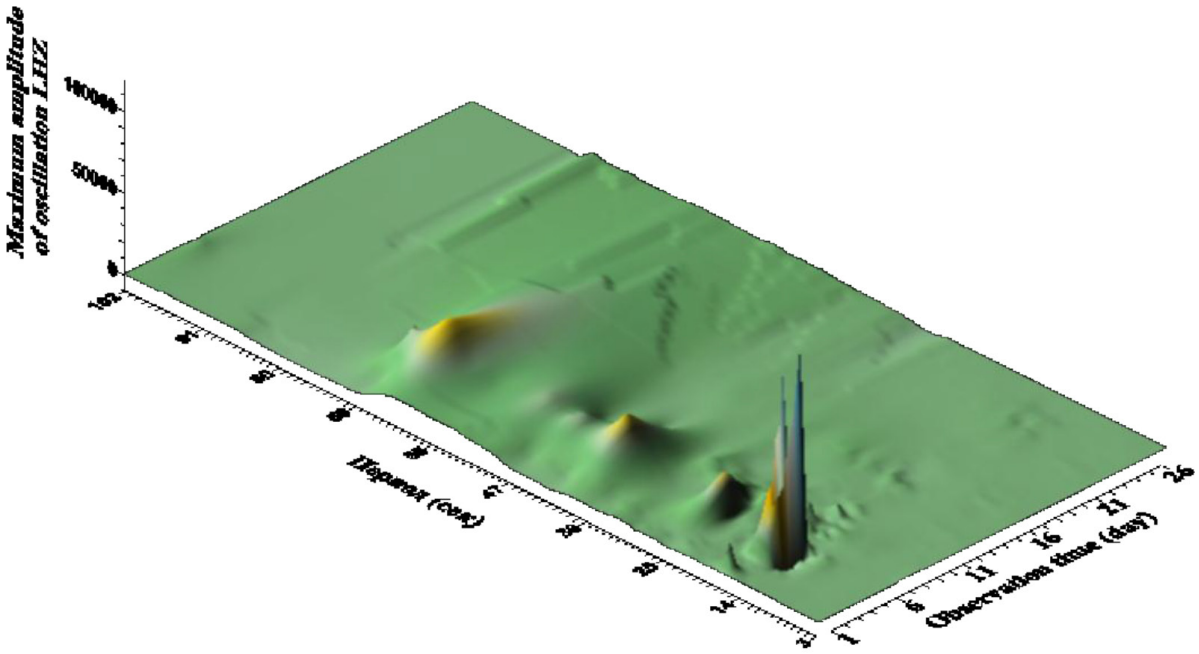

A)

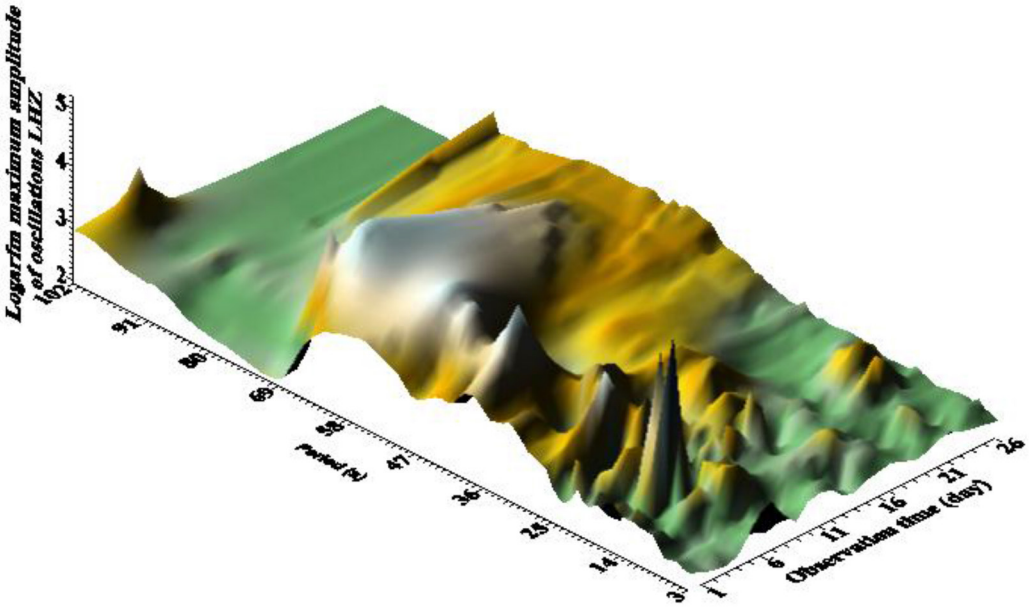

B)

Figure 8. A, B. These are dependence of the maximum amplitude of seismic vibrations A) and its logarithm B), from the observation time and the corresponding period. The interval of the period change is from 2 to 102 sec with a step of 0.1 sec. The time step is 2 minutes (120 seconds). The window is 628 seconds.

According to Fig. 8 (A) for several days, resonant peaks of good quality on micro seismic periods of 14–20 sec can be observed in the wave field; their double period manifests itself in the form of ill-galling small amplitude manifestations. According to Fig. 8 (B) in Antarctica in the general seismic wave field it is possible to distinguish three groups of waves with ranges of periods: relatively high-frequency (periods 3–25 seconds), the longest and with maximum amplitude (periods 49–60 seconds) and short duration of existence as a single peak on period ~ 100 sec. Probably, the longest are associated with existing in the coastal zone and on the shelf of the network of caves and channels (Figure 9).

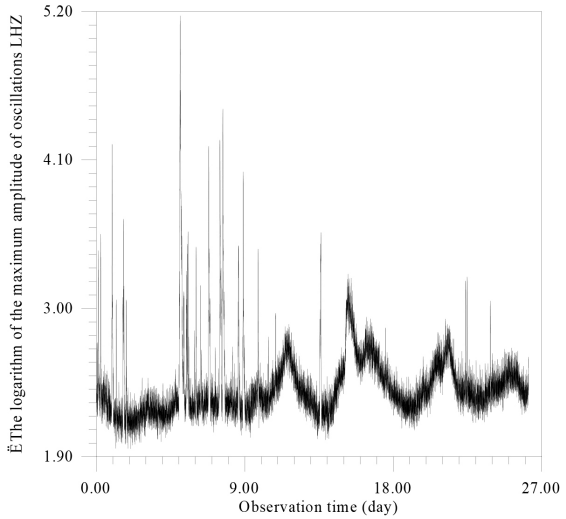

Figure 9. There is the dependence of the logarithm of the maximum amplitude of oscillations on the observation time.

According to Fig. 9, there are two independent types of noise - one high-frequency, constantly existing with an unstable modulation frequency (~ 4–5 days) and the second in the form of very short irregular high-amplitude emissions (Figure 10,11).

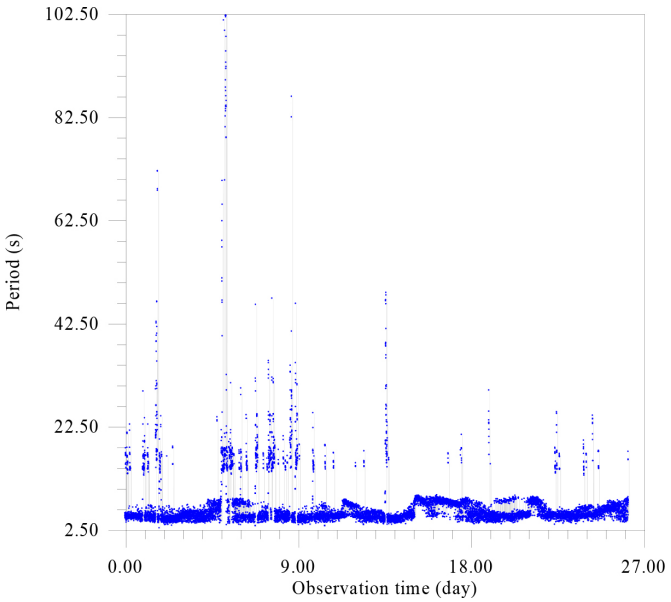

Figure 10. The dependence of the period corresponding to the logarithm of the maximum amplitude of oscillations from the time of observation.

The dependence of the logarithm of the maximum amplitude on the period (Fig. 11) most clearly highlights the zone 3.0 - 7–8.0 s, that is, a known section of storm microseisms. Since such habitual

microseisms are usually recorded, for example, in the Baltic and in Europe, and the geological and structural environment of this region and the Antarctic are fundamentally different, a source of probable general influence should be found. Since high-frequency solar oscillations have a constant activity, especially at periods of 5–6 min, and the lack of ozone protection from the Sun allows for higher frequency effects, these microseisms are inherently strongly associated with solar activity. Another, even more active area lies within 20–25 seconds, which is also recorded in other regions of the Earth (Figure-12).

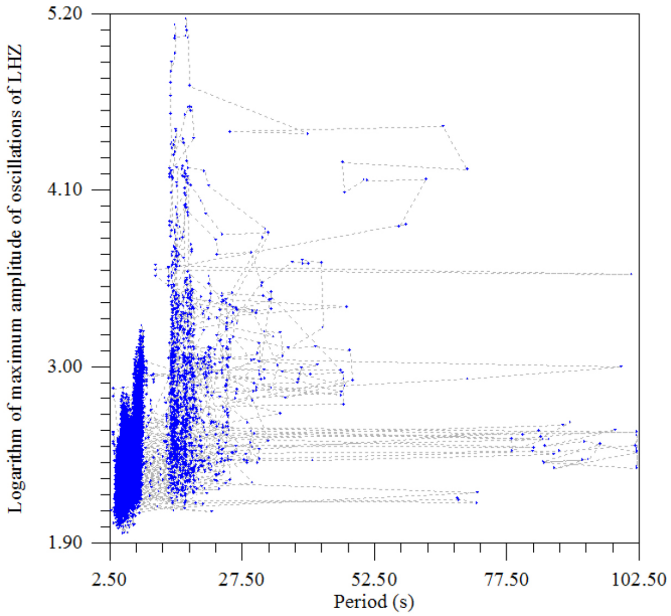

Figure 11. The dependence of the logarithm of the maximum amplitude of oscillations on the period.

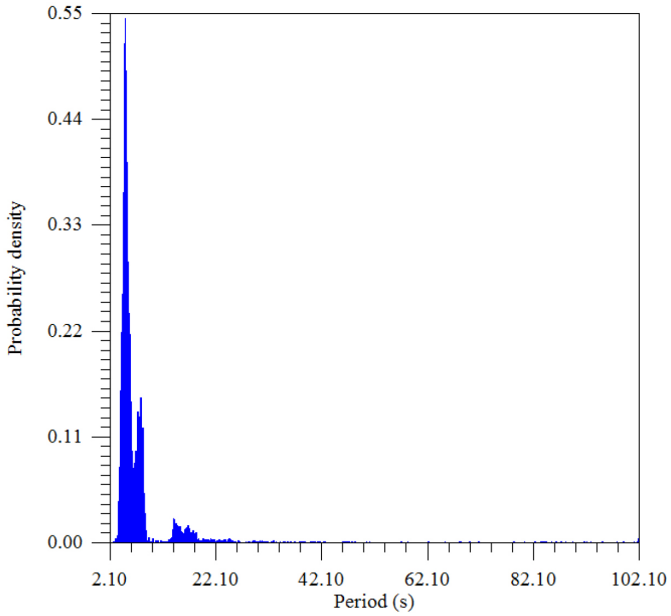

Figure 12. The density distribution of the maximum amplitude of the period.

The distribution of the maximum amplitude over periods divides the seismic vibrations into two groups - powerful ~ 3–6 sec and weak, but connected as resonant harmonics ~ 18–20 sec., which was observed earlier in other regions of the Earth (Figure 13–20).

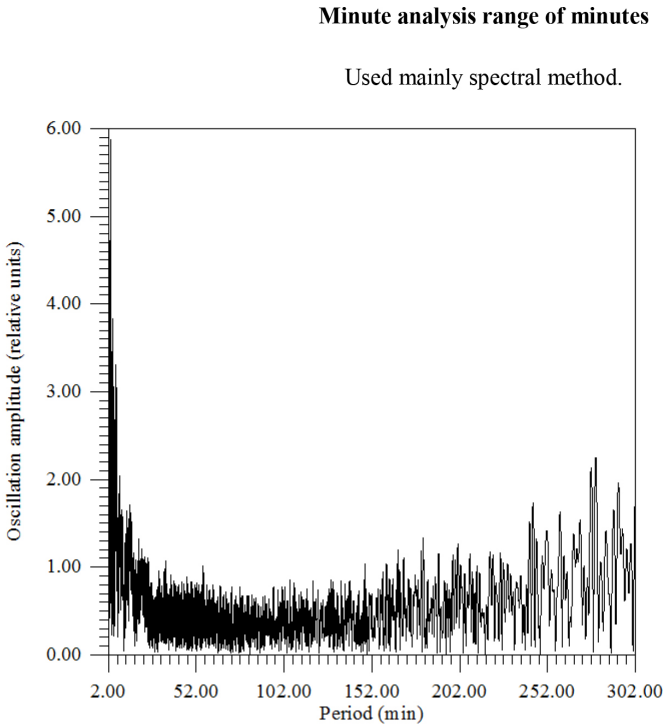

Figure 13. There is amplitude spectrum from 2 to 302 min with a step of 0.03 min.

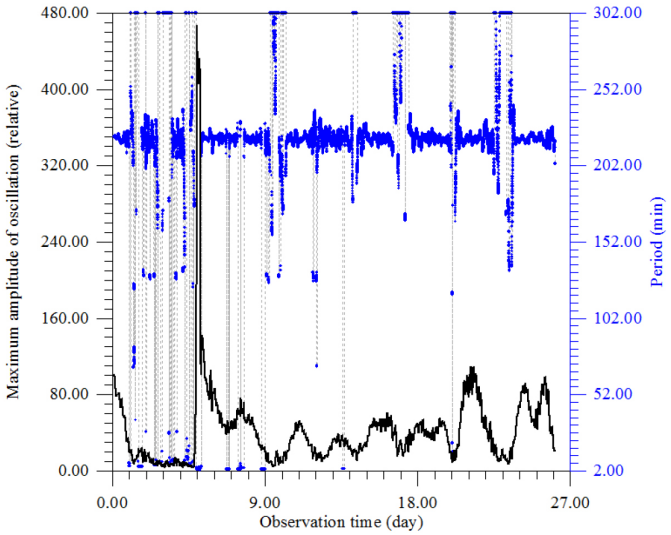

Figure 14. The dependence of the period corresponding to the maximum amplitude of oscillations from the time of observation.

This energy spectrum characterizes the constant component. Therefore, it is still early to draw final conclusions about their reliability and significance. We must try to modify the program a bit, or use the resonance method (Table-2).

This table could also be rebuilt according to a different number of intervals by period. It is noteworthy that in the range of 28÷103 min the number of intervals is very small (Table 3) (Figure 21) (Table 4).

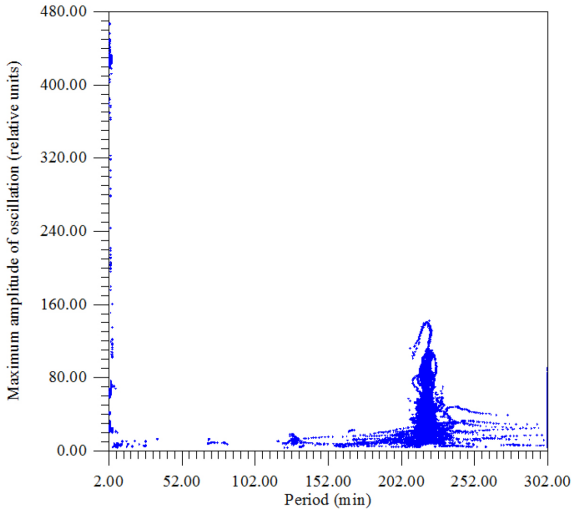

Figure 15. Dependence of the logarithm of the maximum amplitude of oscillations on the period

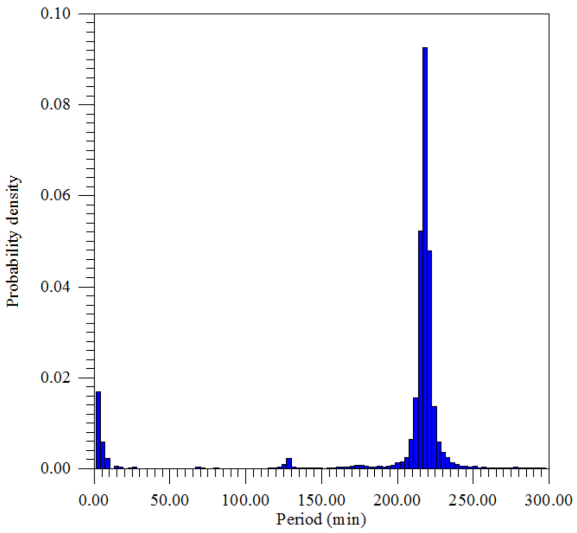

Figure 16. The density distribution of the maximum amplitude of the period.

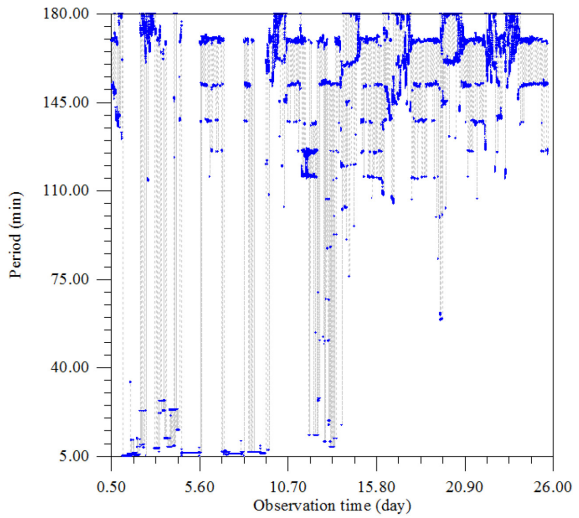

Figure 17. The dependence of the period corresponding to the maximum amplitude of oscillations from the time of observation.

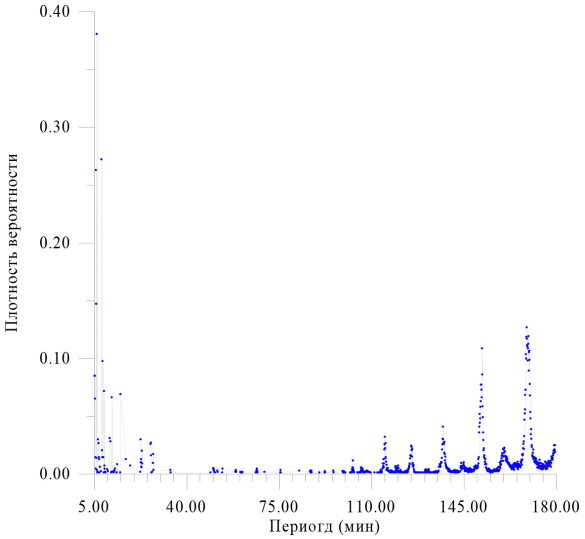

Figure 18. The density distribution of the maximum amplitude of the period.

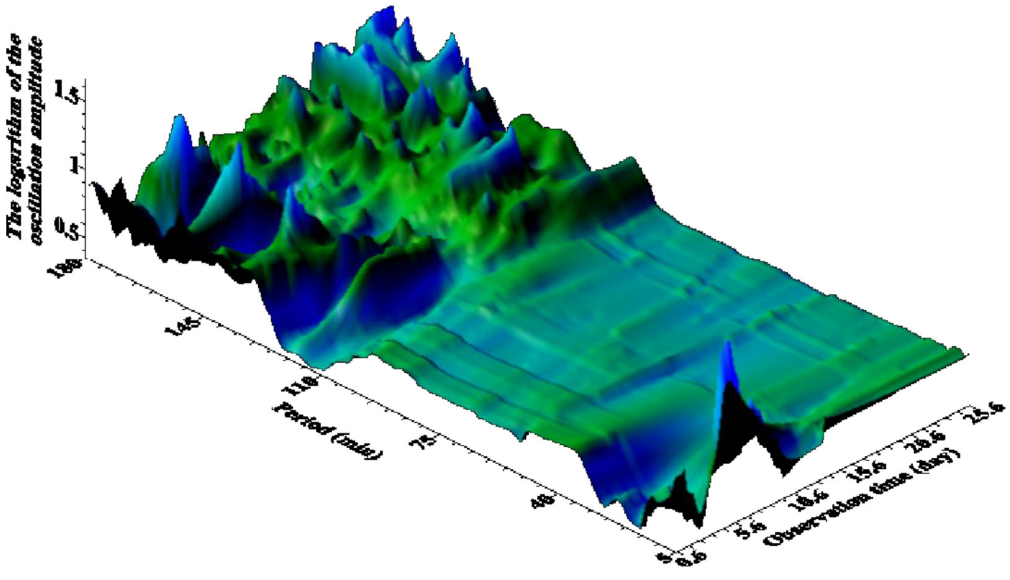

Figure 19. The dependence of the logarithm of the maximum amplitude of oscillations on the time of observation and the corresponding period. The interval of the period is change from 2 to 302 minutes. in 0.3 min steps Time step 2 min. Window - 314 minutes.

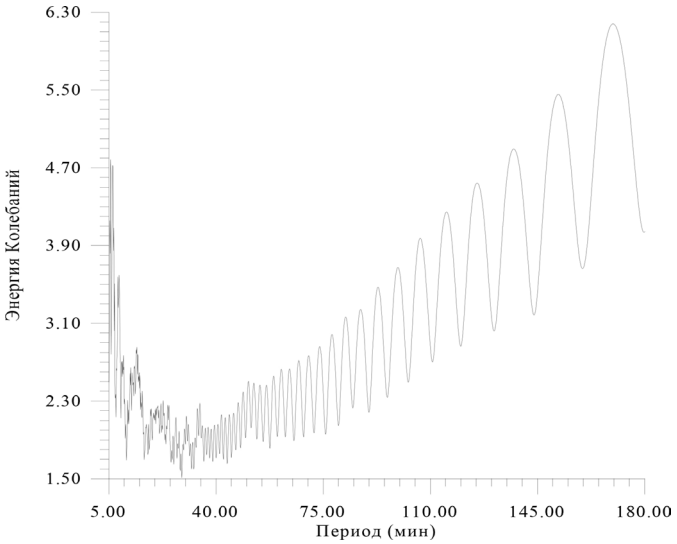

Figure 20. There is energy spectrum data Figure 19.

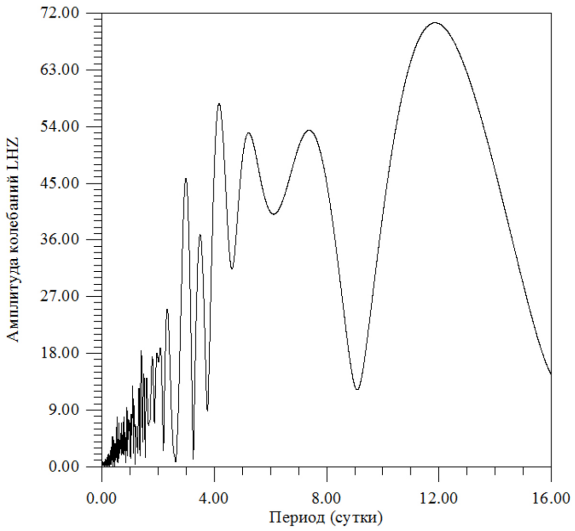

Figure 21. There is amplitude spectrum of the daily range.

Conclusion

As expected, (see Tables 2–4), the structure of the seismic fields of Antarctica is saturated with wave fields determined by cosmic processes, primarily by the Sun's own oscillations (see Table 1). Seismic Antarctica turns it into a unique and indispensable landfill for testing and testing of seismic and geophysical equipment intended for the study of the Moon and planets.

Attachments

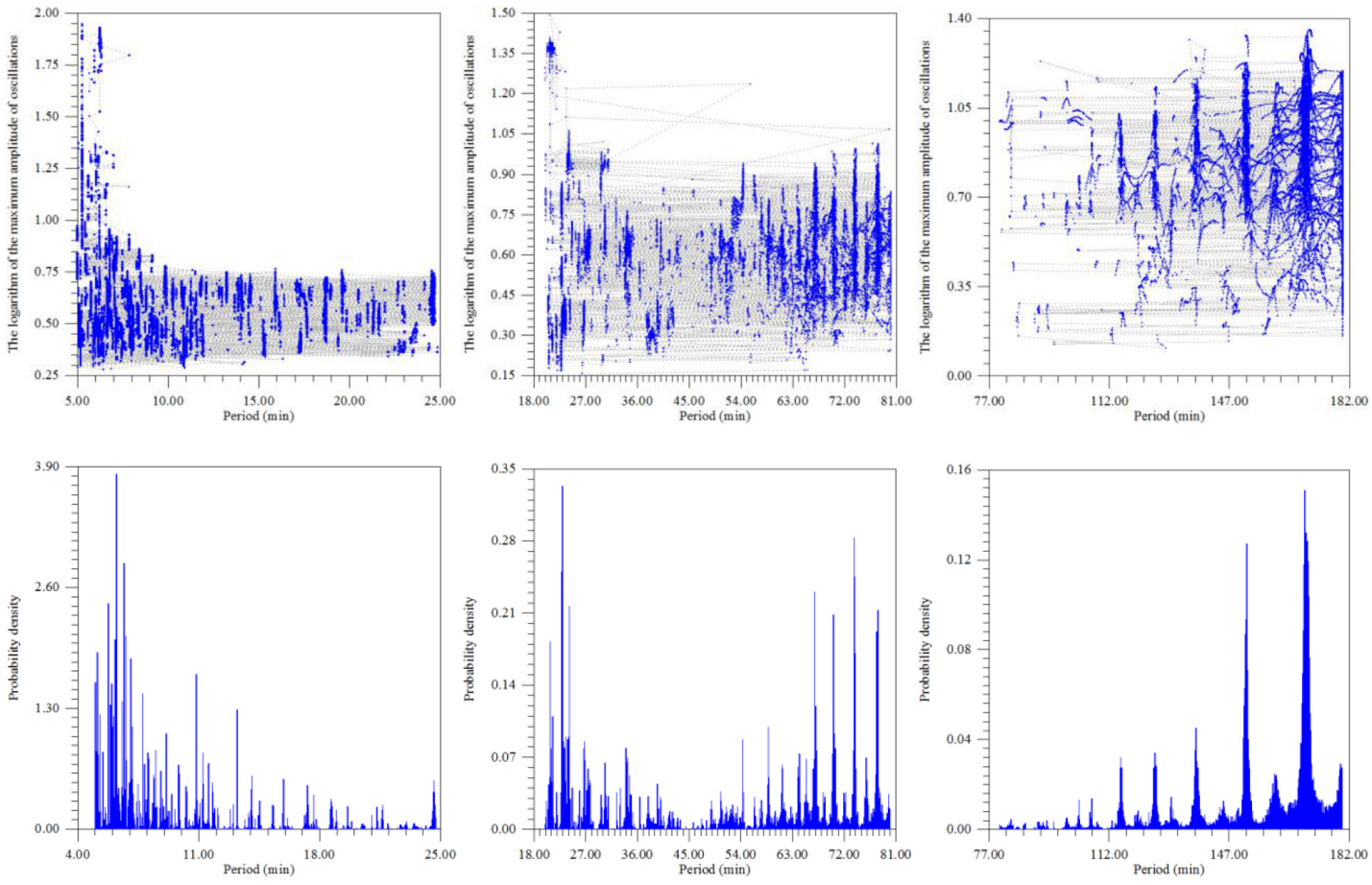

Table 2. Distribution of time intervals for which the periods correspond (N≥10)

Period (min)	N	Period (min)	N	Period (min)	N	Period (min)	N	Period (min)	N	Period (min)	N
5.4002	153	124.5683	11	149.7827	12	161.0891	26	167.6929	30	173.1961	18
5.5003	153	124.6683	10	150.5831	12	161.1892	20	167.7930	39	173.2961	16
5.6003	117	124.7684	15	150.6832	10	161.2893	25	167.8930	46	173.3962	13
5.7004	25	124.8685	14	150.7833	22	161.3893	22	167.9931	50	173.5963	15
5.9005	476	124.9685	23	150.8833	15	161.4894	26	168.0931	38	173.6963	15
6.0006	266	125.0686	28	150.9834	25	161.5894	18	168.1932	58	173.7964	10
6.1006	24	125.1686	28	151.0834	64	161.6895	21	168.2933	84	173.8965	16
6.2007	690	125.2687	27	151.1835	73	161.7895	23	168.3933	94	173.9965	21
6.7010	53	125.3687	43	151.2835	93	161.8896	18	168.4934	100	174.0966	12
6.9011	47	125.4688	36	151.3836	79	161.9897	16	168.5934	123	174.1966	11
7.0011	25	125.5689	41	151.4837	86	162.0897	16	168.6935	131	174.4968	16
7.1012	22	125.6689	26	151.5837	104	162.1898	14	168.7935	187	174.5969	11
7.4014	10	125.7690	38	151.6838	113	162.2898	16	168.8936	180	174.9971	11
8.0017	493	125.8690	16	151.7838	139	162.3899	16	168.9937	214	175.0971	14
8.2018	36	125.9691	13	151.8839	139	162.4899	15	169.0937	229	175.3973	14
8.3019	25	126.0691	12	151.9839	131	162.5900	12	169.1938	211	175.5974	10
8.4019	176	126.1692	10	152.0840	119	162.6901	13	169.2938	201	175.6975	12
8.7021	25	126.2693	13	152.1841	196	162.7901	12	169.3939	199	175.7975	10
9.0023	129	135.8747	10	152.2841	155	162.8902	10	169.4939	177	175.8976	10
9.1023	12	135.9748	10	152.3842	105	163.0903	10	169.5940	196	175.9977	11
11.1035	55	136.0749	10	152.4842	88	163.1903	12	169.6941	203	176.0977	18
11.4037	50	136.1749	14	152.5843	64	163.2904	10	169.7941	215	176.3979	17
11.9039	119	136.2750	10	152.6843	52	163.3905	11	169.8942	161	176.5980	14
13.9051	14	136.3750	12	152.7844	36	163.6906	10	169.9942	190	176.6981	12
15.2058	124	136.4751	10	152.8845	39	163.9908	13	170.0943	192	176.7981	14
17.2070	22	136.5751	15	152.9845	25	164.1909	14	170.1943	178	176.9982	10
18.9079	12	136.6752	17	153.0846	28	164.4911	16	170.2944	140	177.0983	14
22.8102	53	136.7753	17	153.1846	24	164.5911	13	170.3945	122	177.1983	16
22.9102	17	136.8753	17	153.2847	18	164.6912	12	170.4945	96	177.2984	11
23.0103	22	136.9754	24	153.3847	14	164.7913	13	170.5946	86	177.3985	19
23.1103	10	137.0754	37	153.4848	22	164.8913	11	170.6946	61	177.4985	11
23.2104	9	137.1755	45	153.5849	15	164.9914	13	170.7947	69	177.5986	17
23.3105	35	137.2755	54	153.7850	14	165.0914	15	170.8947	54	177.6986	16
23.4105	15	137.3756	73	158.6878	10	165.1915	10	170.9948	44	177.7987	17

Period (min)	N	Period (min)	N	Period (min)	N	Period (min)	N	Period (min)	N	Period (min)	N
26.6123	46	137.4757	53	158.8879	10	165.2915	12	171.0949	41	177.8987	17
26.7124	48	137.5757	47	158.9879	17	165.3916	15	171.1949	27	177.9988	13
26.8125	28	137.6758	47	159.1881	13	165.4917	12	171.2950	28	178.0989	17
27.5129	16	137.7758	46	159.2881	15	165.6918	18	171.3950	32	178.1989	19
27.6129	30	137.8759	32	159.3882	13	165.7918	10	171.4951	25	178.2990	10
103.2561	20	137.9759	49	159.4882	19	165.9919	13	171.5951	37	178.3990	16
114.5626	15	138.0760	30	159.5883	23	166.0920	14	171.6952	22	178.4991	26
114.7627	11	138.1761	20	159.6883	27	166.1921	14	171.7953	23	178.5991	22
114.8627	22	138.2761	26	159.7884	31	166.2921	10	171.8953	25	178.6992	25
115.0629	15	138.3762	16	159.8885	19	166.3922	11	171.9954	18	178.7993	23
115.1629	37	138.4762	13	159.9885	28	166.4922	12	172.0954	24	178.8993	21
115.2630	45	138.5763	11	160.0886	19	166.5923	10	172.1955	24	178.9994	24
115.3630	57	144.1795	11	160.1886	38	166.6923	12	172.2955	17	179.0994	28
115.4631	39	144.2795	16	160.2887	26	166.8925	18	172.3956	20	179.1995	31
115.5631	23	144.4797	10	160.3887	37	166.9925	16	172.4957	24	179.2995	35
115.6632	47	144.9799	11	160.4888	32	167.0926	18	172.5957	16	179.3996	31
115.7633	25	145.0800	12	160.5889	39	167.1926	21	172.6958	22	179.4997	44
115.8633	18	145.1801	14	160.6889	40	167.2927	13	172.7958	15	179.5997	37
116.0634	13	145.2801	17	160.7890	34	167.3927	29	172.8959	14	179.6998	36
119.4654	11	145.3802	11	160.8890	34	167.4928	21	172.9959	18	179.7998	33
120.4659	12	149.2824	10	160.9891	27	167.5929	28	173.0960	9	179.8999	44

Table 3. The distribution of time intervals for which the periods correspond to A_{max}

Period (min)	N	Period (min)	N	Period (min)	N
2.6000	946	146.3120	4	221.1620	2686
5.5940	325	149.3060	4	224.1560	762
8.5880	122	152.3000	1	227.1500	332
11.5820	1	155.2940	9	230.1440	196
14.5760	30	158.2880	13	233.1380	140
17.5700	15	161.2820	18	236.1320	71
20.5640	1	164.2760	17	239.1260	54
23.5580	9	167.2700	25	242.1200	36
26.5520	20	170.2640	36	245.1140	36
32.5400	2	173.2580	42	248.1080	24
68.4680	17	176.2520	44	251.1020	31

Period (min)	N	Period (min)	N	Period (min)	N
71.4620	6	179.2460	26	254.0960	13
74.4560	2	182.2400	20	257.0900	15
77.4500	2	185.2340	18	260.0840	10
80.4440	7	188.2280	33	263.0780	10
116.3720	3	191.2220	22	266.0720	9
119.3660	6	194.2160	35	269.0660	7
122.3600	15	197.2100	47	272.0600	11
125.3540	48	200.2040	71	275.0540	11
128.3480	128	203.1980	86	278.0480	17
131.3420	19	206.1920	135	281.0420	10
134.3360	14	209.1860	359	284.0360	5
137.3300	5	212.1800	868	287.0300	7
140.3240	4	215.1740	2932	290.0240	3
143.3180	6	218.1680	5189	293.0180	6
				296.0120	6

Table 4. The summary of daily periods.

Period (day)	Amplitude fluctuations (rel. units)	Period (day)	Amplitude fluctuations (rel. units)	Period (day)	Amplitude fluctuations (rel. units)
0.00417	2.19146	0.38750	2.34914	0.79306	7.95374
0.00972	1.39646	0.39861	3.12503	0.82917	4.96194
0.11806	1.05268	0.40694	4.69761	0.88750	9.37318
0.13194	1.14954	0.41806	2.71686	0.93750	7.53833
0.13750	1.06967	0.42917	2.80484	0.97639	7.36167
0.16806	1.43672	0.43750	3.39350	1.04583	8.34664
0.18750	1.28783	0.44583	3.64884	1.09583	12.86868
0.20139	1.51607	0.46250	1.25450	1.15139	9.73151
0.20972	1.87710	0.47083	3.53236	1.20972	6.42397
0.22083	1.91259	0.48750	3.70950	1.31806	12.39736
0.22917	2.03499	0.50417	2.77930	1.40139	18.42374
0.24028	2.07343	0.51528	3.61388	1.49028	14.78352
0.25139	1.51939	0.52917	6.31336	1.59306	14.11028
0.26528	1.78014	0.54028	7.88273	1.79306	17.42602
0.28194	1.69116	0.55417	3.96956	1.95972	18.00527
0.29306	1.73287	0.56528	1.75607	2.07917	18.77936

Period (day)	Amplitude fluctuations (rel. units)	Period (day)	Amplitude fluctuations (rel. units)	Period (day)	Amplitude fluctuations (rel. units)
0.29861	2.50799	0.57639	1.94631	2.32639	25.01781
0.30972	2.22962	0.59028	4.55191	2.99028	45.80661
0.31528	2.12205	0.60694	6.98497	3.49583	36.81036
0.32917	2.22865	0.62361	4.12886	4.17083	57.67608
0.33472	3.07918	0.64861	3.80290	5.22083	52.97682
0.35139	2.24693	0.66806	3.72560	7.37917	53.38868
0.35694	4.71118	0.68750	6.98646	11.85972	70.47160
0.37361	2.58232	0.71528	4.98707		
0.38194	3.51410	0.76250	7.11657		

References

1. Khavroshkin OB, Tsyplakov VV (2001) Meteoroid stream impacts on the Moon: information of duration of seismograms // Proc. Conf. Meteoroids 2001 (ESA SP-495). Noordwijk, The Netherlands: *ESA Publ Division* Pg No: 13–21.
2. Khavroshkin OB, Tsyplakov VV (2001) Temporal structure of meteoroid stream and lunar seismicity according to Nakamura's catalogue // Proc. Conf. Meteoroids 2001 (ESA SP-495). Noordwijk, The Netherlands: *ESA Publ. Division* Pg No: 95–105.
3. Khavroshkin OB, Tsyplakov VV, Sobko AA (2011) Solar activity and seismicity of the Moon. *Engineering Physics* 3: 40–45.
4. Christensen Dalsgaard J, Gough DO, Morgan JG (1979) Dirty Solar Models. *Astron. Astrophys* 73: 121–128 .
5. Patrick S. McIntosh, Murray Dryer (1972) Solar activity: observations and predictions. The Massachusetts Institute of Technology, Virginia, USA.
6. Syun-Ichi Akasofu, Sydney Chapman (1972) Solar-Terrestrial Physics. The Clarendon Press, California, USA.
7. Khavroshkin O, Tsyplakov V (2013) Nonlinear Seismology: The Cosmic Component. Saarbrücken: Palmarium Academic Publishing.
8. Oleg Khavroshkin, Vladislav Tsyplakov (2013) Sun, Earth, radioactive ore: common periodicity. *The Natural Science (NS)* 5: 1001–1005.
9. Khavroshkin OB, Tsyplakov VV (2013) Radioactivity, solar neutrinos, interactions. *Engineering Physics* 8: 53–61.
10. Khavroshkin OB, Tsyplakov VV (2013) Ore sample radioactivity: monitoring. *Engineering Physics* 8: 53–62.
11. Khavroshkin OB, Tsyplakov VV (2013) Natural radioactivity as an open system. *Engineering Physics* 12: 40–54.
12. Starodubov AV, Khavroshkin OB, Tsyplakov VV (2014) From periodicities of radioactivity to cosmic and metaphysical oscillations. Metaphysics. Moscow. *Peoples' Friendship University of Russia* 1: 137–149.
13. Rukhadze AA, Khavroshkin OB, Tsyplakov VV (2015) The frequency of natural radioactivity. *Engineering Physics* 5.
14. Khavroshkin OB, Tsyplakov VV (2014) Hydrogen maser: solar periodicity. *Engineering Physics* 3: 25–31.

Citation:

Khavroshkin OB, Khrustalev AB, Tsyplakov VV (2019) Seismicity of Antarctica: features. *Geol Earth Mar Sci* Volume 1(1): 1–12.